Mutations Induced in Tradescantia by Small Doses of X-rays and Neutrons: Analysis of Dose-Response Curves

Abstract. *Dose-response curves for pink somatic mutations in* Tradescantia *stamen hairs were analyzed after neutron and x-ray irradiation with doses ranging from a fraction of a rad to the region of saturation. The dose-effect relation for neutrons indicates a linear dependence from 0.01 to 8 rads; between 0.25 and 5 rads a linear dependence is indicated for x-rays also. As a consequence the relative biological effectiveness reaches a constant value (about 50) at low doses. The observations are in good agreement with the predictions of the theory of dual radiation action and support its interpretation of the effects of radiation on higher organisms. The doubling dose of x-rays was found to be nearly 1 rad.*

The increasing use of atomic energy results in increasing ambient amounts of radiation that could present hazards to man by increasing the incidence of mutations in future generations. Thus, relationships between mutation frequencies and very low doses of radiation should be established. In practice, such studies are difficult to perform with higher organisms because very large populations are required for a statistically significant increase above present background (spontaneous) mutation frequencies to be detected.

Ideally, mammals should be used in studies of radiation effects at low doses so that the data obtained could be extrapolated to man, but this is usually impractical. Certain species of higher plants have been used for radiation studies at very low doses (*1, 2*). Often overlooked is the fact that plants are eucaryotic organisms; because they are, their chromosomes may be similar in structure and basic biochemistry to animal chromosomes. The mechanisms by which ionizing radiation induces mutations or chromosome aberrations, or both, in plants are similar if not identical to the mechanisms in mammals. In addition, very large populations of plants or plant cells often can be grown and analyzed relatively easily. Some plants, such as *Tradescantia* clone 02, are very sensitive to mutation induction by ionizing radiation (*2–4*). Clone 02 is heterozygous for flower color, the normal blue being dominant over the recessive pink. Pink cells or streaks of cells can be seen in mature petals or stamen hairs at appropriate periods after irradiation of young flower buds. The pink cells are herein called mutants although they could presumably also result from chromosome deletions (*5*).

We have studied the shapes of dose-response curves for the pink mutations induced in stamen hair cells by neutrons (0.43 Mev) and x-rays (250 kv-peak). Dose-response curves for the pink mutations and other types of somatic aberrations in clone 02 have been reported for doses of neutrons and x-rays as low as 0.163 and 11.5 rads, respectively (*3, 4*). We report additional experiments at still lower doses and show that the results are in accord with the theory of dual radiation action (*6*).

For details of the experimental procedures see (*4*). Young cuttings of *Tradescantia* clone 02 bearing young flower buds were used. Stock plants and cuttings were grown in controlled-environment growth chambers with an 18-hour day, an illuminance of 18,150 lu/m^2, and temperatures of 20° and 17.8°C in the daytime and at night, respectively.

All irradiations and scorings were done at Brookhaven National Laboratory. The stamen hairs were scored from day 11 to day 15 after irradiation, when the mutation frequency is known to reach peak values. Data from all earlier experiments (1 and 5 in Table 1) (*3, 4*) were recomputed to incorporate only the data from these days of scoring.

The neutron irradiations were performed at the Radiological Research Accelerator Facility at Brookhaven (*7*). The x-radiations were administered at 30 rad/min for doses down to 6 rads; below this dose, for practical considerations, the dose rate was 1 rad/min. A check at 6 rads for both dose rates did not reveal a dose-rate effect.

Table 1 gives the neutron and x-ray doses, the resulting frequencies of pink-mutant events per stamen hair, the standard deviations, the numbers of stamen hairs, and the number of mutant events scored for each exposure. The average mutation frequencies (total mutant events divided by total hairs) observed during the 5-day scoring period are graphed logarithmically in Fig. 1.

All the neutron data (0.01 to 8 rads) can be fitted to a straight line of slope +1. The mutation frequency at 10

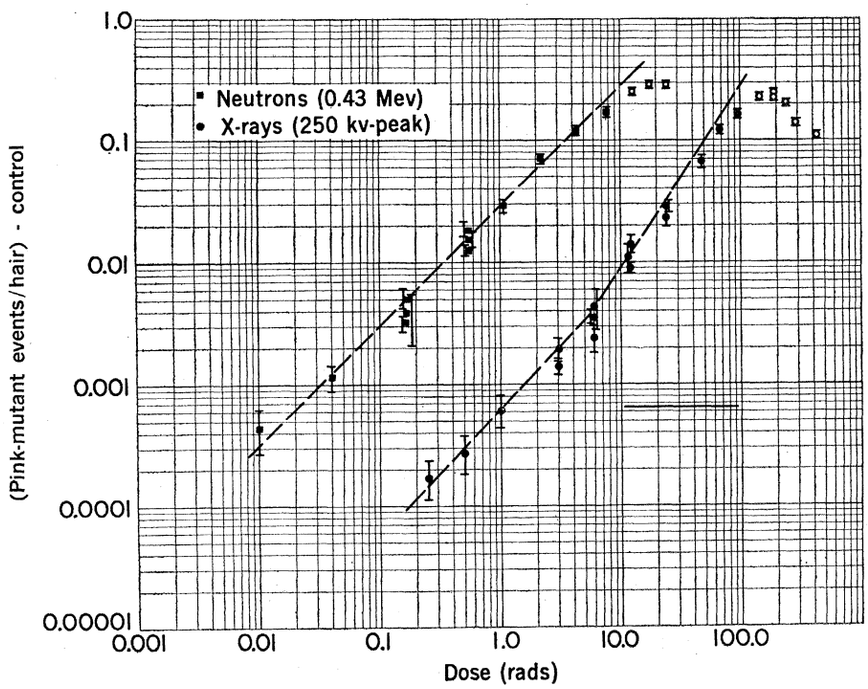

Fig. 1. Neutron and x-ray dose-response curves for pink-mutant events in stamen hairs of *Tradescantia* clone 02. The points represent average values obtained by dividing the total number of mutant events by the total number of stamen hairs scored from day 11 through day 15 after irradiation, when the mutation frequency is highest. The open symbols are saturation points and were not used in computing the true slopes. The dashed lines represent slopes based on equations and computations given in the text. The horizontal line indicates the mutant-event frequency in control experiments.

mrad is somewhat high, but it lies on the line within the experimental error. Also, it is difficult to see how a departure from linearity can occur when the particle event frequency (average number of charged particles traversing the cell) is much less than one. The apparent curvilinearity of the x-ray line can be approximated by two straight-line segments, one with slope +1.4 from about 5 to 100 rads, the other with slope +1 from 0.25 to 6.0 rads. A *t*-test indicates that these slopes are significantly different ($P < .01$). However, a more meaningful interpretation is that the entire ascending portion of the x-ray curve can be fitted as the sum of a linear and a quadratic dose term.

From 5.0 to 100 rads, relative biological effectiveness (RBE) decreases with increasing x-ray dose from about 50 to about 15. Thus, with higher doses x-rays become more efficient per rad relative to neutrons. Below x-ray doses of 5 rads, the RBE does not increase indefinitely but remains constant at about 50. The high RBE may be, in part, due to the large chromosomes characteristic of many *Tradescantia* species.

There is no sign of a threshold in either the neutron or x-ray curves. Hence, a response would probably be observable at still lower doses, but it would be a formidable task to undertake such experiments, especially with x-rays, because several million stamen hairs would have to be scored. However, such experiments are feasible.

It has been pointed out (*8*) that for a variety of radiation effects on higher organisms the RBE of neutrons relative to x-rays increases with decreasing dose. The functional dependence of RBE on dose is the point of departure of the theory of dual radiation action (*6*), which predicts that the RBE must become constant at very low doses. The observations reported here represent a clear-cut example of this.

According to the dual action theory, radiation effects on higher organisms are due to elementary lesions that are produced at a rate, ϵ, which depends on the square of the specific energy (*9, 10*), z, in nuclear regions of the cell with dimensions of the order of 1 μm. A mathematical expression of this relation for x-rays and neutrons is:

$$\epsilon_X = K[(\bar{z}_D)_X D_X + D_X^2]$$
$$\epsilon_N = K[(\bar{z}_D)_N D_N + D_N^2]$$

where K is a constant, $\bar{z}_D$ is the dose average of specific energy increments, and D is the absorbed dose.

The dependence of mutation frequency on dose for neutrons indicates that for this radiation $\bar{z}_D \gg D$, but in the case of x-rays these quantities appear to be comparable within the dose range investigated. From the facts that the RBE (D_X/D_N when $\epsilon_X = \epsilon_N$) at low doses tends to the value $(\bar{z}_D)_N/(\bar{z}_D)_X = 54$ and that $(\bar{z}_D)_X = D_X$ when the RBE is 27 (a result obtained by substitution) one can readily derive that $(\bar{z}_D)_N = 970$ rads and $(\bar{z})_X = 18$ rads. These values occur when d, the diameter of the volume in which the energy concentration is critical, is about 2 μm. The value of K is about 3.1×10^{-5} rad^{-2}. It depends on the choice of mutation frequency, among other factors. When the values are substituted in the above equations the two dashed lines in Fig. 1 are obtained. There is good agreement between theory and experiment in the ascending portions of the dose-response curves. The descending portions are due to another factor or factors, possibly cell killing.

In view of a common tendency to estimate radiation hazards on the basis of extrapolations, we give the frequency of mutations in our control experiments. It is represented by the horizontal line at about 6.5×10^{-4} events per hair in Fig. 1. (Experiment 7 had the largest sample.) The "doubling dose" for x-rays is thus nearly 1 rad—a value considerably less than that ob-

Table 1. Frequencies of pink-mutant events in stamens of *Tradescantia* clone 0.2. The values are averages obtained by dividing the total number of mutant events by the total number of stamen hairs scored from day 11 to day 15 after irradiation. The control frequencies were subtracted from the frequencies obtained in radiation experiments.

Dose (rads)	Experiment	Mutant events per hair	S.D.	Total mutant events	Total stamen hairs scored
		Neutrons (0.43 Mev)			
Control	1	0.0015	0.0008	4	2,636
Control	2	0.0006	0.0004	2	3,395
Control	3	0.0007	0.0001	61	87,320
0.01	3	0.00044	0.00017	109	95,729
0.04	3	0.00115	0.00025	69	37,278
0.163	1	0.0038	0.0017	14	2,621
0.163	2	0.0050	0.0013	19	3,407
0.163	3	0.0032	0.0005	123	31,559
0.54	1	0.0183	0.0032	47	2,371
0.54	2	0.0156	0.0024	55	3,385
0.54	3	0.01288	0.00122	350	25,778
1.07	1	0.0296	0.0038	73	2,349
2.16	1	0.0693	0.0058	161	2,275
4.34	1	0.1203	0.0076	285	2,339
7.94	1	0.1765	0.0089	423	2,377
7.94	2	0.1771	0.0074	661	3,720
12.70	1	0.2558	0.0106	603	2,344
17.20	1	0.2940	0.0113	687	2,325
24.40	1	0.2910	0.0108	679	2,321
		X-rays (250-kv peak)			
Control	4	0.0035	0.0018	5	1,431
Control	5	0.0029	0.0012	6	2,094
Control	6	0.00087	0.00011	72	82,972
Control*	7	0.00065	0.00007	622	938,408
0.25†	7	0.000167	0.000064	820	960,698
0.5	7	0.00027	0.00010	182	189,970
1.0	6	0.00063	0.00019	137	91,346
3.0	6	0.00195	0.00039	80	28,354
3.0	7	0.00138	0.00018	112	55,432
6.0	6	0.00365	0.00048	138	30,564
6.0	2	0.0044	0.0015	17	3,374
6.0	7	0.0024	0.0006	144	42,076
11.5	5	0.0111	0.0031	27	1,929
12.0	6	0.00882	0.00075	292	30,139
12.0	2	0.0145	0.0024	55	3,634
24.0	5	0.0241	0.0040	51	1,886
24.0	2	0.0298	0.0032	106	3,484
48.0	5	0.0682	0.0066	135	1,900
68.0	2	0.1253	0.0066	438	3,480
96.0	5	0.1624	0.0096	301	1,821
144.0	5	0.2301	0.0104	480	2,060
192.0	5	0.2262	0.0101	476	2,078
192.0	4	0.2453	0.0059	1900	7,636
240.0	5	0.2030	0.0101	391	1,899
288.0	5	0.1413	0.0086	297	2,059
432.0	5	0.1096	0.0076	223	1,982

* Two-part experiment in which 402,548 and 535,860 stamen hairs were scored. The frequency was used as the control value in Fig. 1. † Two-part experiment in which 399,722 and 560,976 stamen hairs were scored.

served for certain effects in mammalian systems such as mice (*11*)—and the dose-effect curve departs from linearity when the frequency of radiation-induced mutations is only about five times the spontaneous frequency. This underlines the deficiencies of linear extrapolations from large effects. For example, the mutation frequency at 1 rad, estimated from the mutation frequency at 50 rads, would be more than twice as much as the observed rate.

A. H. SPARROW

Biology Department,
Brookhaven National Laboratory,
Upton, New York 11973

A. G. UNDERBRINK
H. H. ROSSI

Department of Radiology, Radiological Research Laboratories, College of Physicians and Surgeons, Columbia University, New York 10032

References and Notes

1. L. Ehrenberg and G. Eriksson, *Acta Radiol. Suppl.* **254**, 73 (1966); G. Eriksson, *Hereditas* **68**, 101 (1971); D. Lindgren, G. Eriksson, L. Ehrenberg, *Mutat. Res.* **10**, 335 (1970); G. G. Nayar, K. P. George, A. R. Gopal-Ayengar, *Radiat. Bot.* **10**, 287 (1970); A. H. Sparrow and W. R. Singleton, *Amer. Natur.* **87**, 29 (1953); A. H. Sparrow, R. L. Cuany, J. P. Miksche, L. A. Schairer, *Radiat. Bot.* **1**, 10 (1961).
2. L. W. Mericle and R. P. Mericle, *Radiat. Bot.* **5**, 475 (1965); *Health Phys.* **11**, 1607 (1965).
3. A. G. Underbrink, R. C. Sparrow, A. H. Sparrow, H. H. Rossi, *Radiat. Res.* **39**, 463 (1969).
→ ———, *ibid.* **44**, 187 (1970); *Int. J. Radiat. Biol.* **19**, 215 (1971).
5. L. W. Mericle and R. P. Mericle, *Radiat. Bot.* **7**, 449 (1967).
→ A. M. Kellerer and H. H. Rossi, *Radiat. Res.* **47**, 15 (1971).
7. L. J. Goodman and U. Koch, *Annual Report on Research Project NYO-2740-6* (Department of Radiology, Radiological Research Laboratories, Columbia University, New York, 1969), p. → H. H. Rossi, J. L. Bateman, V. P. Bond, L. J. Goodman, E. E. Stickley, *Radiat. Res.* **13**, 503 (1960).
8. H. H. Rossi, *Phys. Med. Biol.* **15**, 255 (1970).
9. The absorbed dose is defined as $D = E/m$, where E is the energy deposited by charged particles in mass m. However, microscopic regions of diameter d and mass μ exhibit a range of specific energy $z = \epsilon/\mu$, where ϵ is a (generally) highly variable local energy deposition. The probability distribution of increments of specific energy is $f_1(z)$; $\bar{z}_D$ is the ratio of the second and first moments of this distribution (*10*).
10. H. H. Rossi, *Advan. Biol. Med. Phys.* **11**, 27 (1967); A. M. Kellerer and H. H. Rossi, *Proc. Symp. Microdosim. 2nd*, 841 (1969).
11. K. G. Lüning and A. G. Searle, *Mutat. Res.* **12**, 291 (1971).
12. We thank the many technicians and summer students at Brookhaven who helped score the stamen hairs and, in particular, D. Sautkulis, R. C. Sautkulis, and L. A. Schairer for their technical involvement with the lower dose exposures; L. J. Goodman and S. Marino, who assisted with the development of irradiation arrangements and performed the neutron dosimetry; K. H. Thompson, who developed the necessary computer programs; Dr. A. Kellerer, V. Pond, and R. C. Sparrow for suggestions concerning the manuscript. Supported in part by the U.S. Atomic Energy Commission; PHS, Bureau of Radiological Health, grant RL 00074-11; PHS grant CA-12536 from the National Cancer Institute; and NASA purchase order A-44246A.

8 December 1971; revised 31 January 1972

Hydroxyproline Heterooligosaccharides in Chlamydomonas

Abstract. *Most of the hydroxyproline in* Chlamydomonas reinhardtii *is glycosidically linked to oligosaccharides and a monosaccharide that are different from the arabinosides found in hydroxyproline-containing plant cell walls previously examined. Of particular interest is the presence of hydroxyproline-*O*-galactose. These differences may be common to the volvocalean green algae and may be related to lower tensile strength of the cell walls of this group of plants.*

In the search for a cell wall component capable of regulating cell wall extensibility, the hydroxyproline-rich protein extensin features as a possible candidate because of its ability to cross-link polysaccharides through the hydroxyproline-*O*-arabinose linkage (*1*). This linkage is detected by the appearance of a series of hydroxyproline arabinosides (Hyp-Ara_n, where $n = 1$ to 4) released from the cell wall by alkaline hydrolysis. These arabinosides have been isolated from all plants examined, ranging from the spermatophytes to the green alga *Chlorella* (*1*, *2*). Especially remarkable in the survey (*2*) was the constancy of arabinose as the only hydroxyproline substituent, with a limit of four arabinose residues.

This survey has been extended to *Chlamydomonas*, an organism considered phylogenetically to be more primitive than *Chlorella*. We now report that alkaline hydrolysis of a crude cell wall fraction from *Chlamydomonas* releases a striking variety of hydroxyproline-*O*-glycosides. These include hydroxyproline-*O*-galactose observed in nature for the first time and a number of hydroxyproline heterooligosaccharides.

Cells of *Chlamydomonas reinhardtii* (IUCC 89) were grown in 12-liter flasks containing 6 liters of Sager and Granick's acetate medium (*3*). Cultures were bubbled continuously with air and maintained under a bank of six fluorescent tubes yielding an intensity of 33,000 lu/m^2. Cells were harvested by centrifugation at the end of the logarithmic growth phase, washed with sterile water, resuspended in water, and sonicated at the maximum setting for 20 minutes (Branson Sonic Power Sonifier). Microscopic examination showed that this treatment completely shattered all cells. The homogenate was made to 10 percent with trichloroacetic acid and centrifuged at 5000*g* for 20 minutes. The pellet was resuspended in water, neutralized with KOH, and sedimented again, yielding a crude fraction containing the cell walls. Alkaline hydrolysis [0.2*M* $Ba(OH)_2$ for 6 hours at 100°C] of this fraction yielded a mixture of hydroxyproline glycosides, which were separated chromatographically on a column (0.6 by 75 cm) of Chromobeads B (Technicon Corp.) and monitored for hydroxyproline by automated analysis as described (*2*), except that a 0 to 0.2*N* HCl gradient was used to improve the resolution of the hydroxyproline glycosides (Fig. 1). The glycosides were hydrolyzed in 2*N* trifluoroacetic acid (*4*). Sugars from the hydrolyzates were identified by paper chromatography in ethyl acetate, pyridine, water (8 : 2 : 1) solvent (*5*) and development with alkaline silver nitrate (*6*). These identifications were confirmed by gas chromatography of the sugar alditol acetates (*4*). Amino acids other than hydroxyproline were assayed for by paper electrophoresis (*7*). The hydroxyproline, arabinose, and galactose were estimated (*7*), and glucose was estimated with Glucostat (an enzymic assay obtained from Worthington Biochemical).

For determination of the sequence of sugars, each glycoside was partially hydrolyzed in 0.1*N* trifluoroacetic acid at 90°C for 0.5 hour. This mild acid hydrolysis released a mixture of hydroxyproline glycosides as breakdown products of the original hydroxyproline glycosides. Separation and analysis of these glycosides enables us to determine a tentative sugar sequence.

Figure 1 shows the profile of hydroxyproline glycosides eluted from the

Table 1. Composition of hydroxyproline (Hyp) glycosides from *Chlamydomonas reinhardtii*.

Glycoside	Hyp (% of total)	Theoretical* molar ratios of glycosides
Hyp A_1	12.7	Ara_5-Gal_5-Glc_2-Hyp
Hyp A_2	4	
Hyp B	12.3	Ara_3-Gal-Glc-Hyp
Hyp C	17.6	Ara_3-Gal-Glc-Hyp
Hyp D	12.6	Ara_3-Gal-Hyp
Hyp E	13	Ara_3-Gal-Hyp
Hyp F	6.2	Ara_2-Gal-Hyp
Hyp G	10.8	Ara_2-Gal-Hyp
Hyp H	0.9	Ara_2-Hyp
Hyp I	4.1	Gal-Hyp
Hyp J	2.4	Gal-Hyp
Hyp K	1	Ara-Hyp
Free Hyp	2.4	*trans* and *cis* Hyp

* For estimated molar ratios, see Table 2.